A Semi-implicit Backward Differentiation ADI Method for Solving Monodomain Model*

Maryam Alqasemi[1] and Youssef Belhamadia[2][0000−0003−2712−564X]

[1] American University of Sharjah, Department of Mathematics, Sharjah, United Arab Emirates.
[2] American University of Sharjah, Department of Mathematics, Sharjah, United Arab Emirates. ybelhamadia@aus.edu

Abstract. In this paper, we present an efficient numerical method for solving the electrical activity of the heart. We propose a second order alternating direction implicit finite difference method (ADI) for both space and time. The derivation of the proposed ADI scheme is based on the semi-implicit backward differentiation formula (SBDF). Numerical simulation showing the computational advantages of the proposed algorithm in terms of the computational time and memory consumption are presented.

Keywords: Monodomain Model · SBDF methods · ADI methods · Mitchell–Schaeffer Model · Spiral Wave.

1 Introduction

Mathematical modeling of biological activities has been proven to be of high importance in the modern computer age. It is an alternative tool to live experiments and can provide solutions to several biomedical problems. In electrocardiology, the most used mathematical models are the bidomain and monodomain models. The monodomain is considered as a simplified version of the bidomain model and although it lacks physiological foundation, it is widely used in the computational electrophysiology community.

Mathematically, the monodomain model consists of a single parabolic partial differential equation coupled with a system of nonlinear ordinary differential equations modeling cell ionic activity. Solving the monodomain model requires fine meshes and small time-steps as the cardiac electrical wave has a stiff wave front, which makes the numerical simulation challenging. In the literature, there are many methods to reduce the computational challenges of both the bidomain and monodomain models. The spatial and temporal discretization effects in cardiac electrophysiology have been numerically investigated in [1] and [2]. Anisotropic mesh adaptation techniques are presented in [3–5]. Operator splitting and high-order methods have been studied in [6–9] and parallel algorithms for cardiac models have been investigated in [10–12].

* The authors acknowledge the financial support of the American University of Sharjah for the Enhanced Faculty Research Grant.

ICCS Camera Ready Version 2021
To cite this paper please use the final published version:
DOI: 10.1007/978-3-030-77977-1_43

Recently, we demonstrated the efficiency of alternating direction implicit (ADI) finite difference methods for solving the monodomain model [13]. The computational advantages of ADI methods have been demonstrated in comparison with the standard finite difference method. The derivation of the ADI methods in [13] was based on the semi-implicit Crank–Nicolson/Adams–Bashforth (CNAB) scheme. The main goal of this paper is to derive an ADI scheme based on the semi-implicit backward differentiation formula (SBDF). The proposed method will be referred to as SBDF-ADI scheme. The semi-implicit methods, especially SBDF type methods, are considered among the best schemes for solving the bidomain and monodomain models (see [2] and [14]). The SBDF schemes enable higher order time stepping that is needed for accurate numerical simulations of the electrical waves of the heart.

In this paper, a second order SBDF-ADI method for the monodomain model is derived. In Section 2, both SBDF and SBDF-ADI schemes are illustrated in the two-dimensional case. In Section 3, numerical results are presented to demonstrate the order of convergence and the computational advantages of the proposed scheme in terms of the computational time and memory consumption. In all our simulations, a comparison with the standard SBDF finite difference method is presented.

2 Derivation of SBDF-ADI Method

2.1 Two-dimensional SBDF Method

The main governing equations of the monodomain model are given by the following system

$$\begin{cases} \dfrac{\partial V_m}{\partial t} - \nabla \cdot (\boldsymbol{D} \nabla V_m) = I_{ion}(V_m, \boldsymbol{W}), \\ \dfrac{\partial \boldsymbol{W}}{\partial t} = g(V_m, \boldsymbol{W}). \end{cases} \tag{1}$$

Where V_m is the trans-membrane potential, $\boldsymbol{W}$ is the cellular states, and $\boldsymbol{D} = \text{diag}(D_x, D_y)$ is the conductivity tensor. The functions $I_{ion}(V, \boldsymbol{W})$, and $g(V, \boldsymbol{W})$ represents the single cell model. Before we derive the SBDF-ADI method, we first present the second-order SBDF scheme by re-expressing the system (1) in the following vector form:

$$\frac{\partial \boldsymbol{U}}{\partial t} = A\boldsymbol{U} + F(\boldsymbol{U}), \tag{2}$$

where

$$\boldsymbol{U} = \begin{pmatrix} V \\ \boldsymbol{W} \end{pmatrix}, \quad A = \begin{pmatrix} D_x \dfrac{\partial^2}{\partial x^2} + D_y \dfrac{\partial^2}{\partial y^2} & \mathbf{0} \\ \mathbf{0} & \mathbf{0} \end{pmatrix} \text{ and } F(\boldsymbol{U}) = \begin{pmatrix} I_{ion}(V, \boldsymbol{W}) \\ g(V, \boldsymbol{W}) \end{pmatrix}.$$

The second-order SBDF requires to start from $\boldsymbol{U}^{n-1}$ at time t^{n-1} and $\boldsymbol{U}^n$ at time t^n as follows:

ICCS Camera Ready Version 2021
To cite this paper please use the final published version:
DOI: 10.1007/978-3-030-77977-1_43

$$\frac{3\boldsymbol{U}^{n+1} - 4\boldsymbol{U}^{n} + \boldsymbol{U}^{n-1}}{2\Delta t} = A\boldsymbol{U}^{n+1} + 2F(\boldsymbol{U}^{n}) - F(\boldsymbol{U}^{n-1}) \tag{3}$$

Using finite difference method, the continuous space domain must be discretized into a mesh with a finite number of grid points. To ensure second order in space, we use the second-order central difference in all our numerical results. For the two-dimensional case, the scheme (3) requires solving a linear system of size $((M+1)^2, (M+1)^2)$, where M is the number of spatial steps. The main idea about ADI-type method is to reduce this system to series of a linear system of size $((M+1), (M+1))$ as is presented in the next subsection.

2.2 Two-dimensional SBDF-ADI Method

To derive the two-dimensional SBDF-ADI algorithm proposed in this study, we must first re-express system (2) as follows

$$\frac{\partial \boldsymbol{U}}{\partial t} = A_1\boldsymbol{U} + A_2\boldsymbol{U} + F(\boldsymbol{U}), \tag{4}$$

where

$$A_1 = \begin{pmatrix} D_x\dfrac{\partial^2}{\partial x^2} & \mathbf{0} \\ \mathbf{0} & \mathbf{0} \end{pmatrix} \text{ and } A_2 = \begin{pmatrix} D_y\dfrac{\partial^2}{\partial y^2} & \mathbf{0} \\ \mathbf{0} & \mathbf{0} \end{pmatrix}.$$

The SBDF system (3) is therefore written as

$$\frac{3\boldsymbol{U}^{n+1} - 4\boldsymbol{U}^{n} + \boldsymbol{U}^{n-1}}{2\Delta t} = A_1\boldsymbol{U}^{n+1} + A_2\boldsymbol{U}^{n+1} + 2F(\boldsymbol{U}^{n}) - F(\boldsymbol{U}^{n-1}) \tag{5}$$

Rearanging (5) by taking $\boldsymbol{U}^{n+1}$ terms in one side and the rest terms in the other:

$$\left(I - \frac{2\Delta t}{3}A_1 - \frac{2\Delta t}{3}A_2\right)\boldsymbol{U}^{n+1} = \frac{4}{3}\boldsymbol{U}^{n} - \frac{1}{3}\boldsymbol{U}^{n-1} + \frac{2\Delta t}{3}\left(2F(\boldsymbol{U}^{n}) - F(\boldsymbol{U}^{n-1})\right). \tag{6}$$

The main idea for ADI is to use a perturbation of this equation. In our case, the perturbed form used is

$$\left(I - \frac{2\Delta t}{3}A_1\right)\left(I - \frac{2\Delta t}{3}A_2\right)\boldsymbol{U}^{n+1} = \frac{4}{3}\boldsymbol{U}^{n} - \frac{1}{3}\boldsymbol{U}^{n-1} + \frac{2\Delta t}{3}\left(2F(\boldsymbol{U}^{n}) - F(\boldsymbol{U}^{n-1})\right). \tag{7}$$

Both equations, (3) and (7), are equivalent and preserve the same time order of accuracy. Now, based on the Douglas–Gunn time splitting scheme, our

ICCS Camera Ready Version 2021
To cite this paper please use the final published version:
DOI: 10.1007/978-3-030-77977-1_43

proposed SBDF-ADI scheme consists of the following system of equations:

$$\begin{cases} \left(I - \dfrac{2\Delta t}{3}A_1\right)\boldsymbol{U}^* = \dfrac{\Delta t}{3}A_2\boldsymbol{U}^n + \dfrac{4}{3}\boldsymbol{U}^n - \dfrac{1}{3}\boldsymbol{U}^{n-1} + \dfrac{2\Delta t}{3}\left(2F(\boldsymbol{U}^n) - F(\boldsymbol{U}^{n-1})\right), \\ \left(I - \dfrac{2\Delta t}{3}A_2\right)\boldsymbol{U}^{n+1} = \boldsymbol{U}^* - \dfrac{2\Delta t}{3}A_2\boldsymbol{U}^n. \end{cases} \tag{8}$$

The second-order central difference is used for spatial discretization. Each linear system corresponding to each spatial direction in this scheme is of size $((M+1),(M+1))$, which allows a great gain in the computational time as is presented in the next section.

All the simulations were performed using MATLAB. All the linear systems obtained in this paper were solved by using decomposition MATLAB built-in function. This function returns the same results as mldivide (backslash operator) but in a much faster way for the presented iterative algorithms. All our MATLAB functions are optimized compared to our previous work presented in [13].

3 Numerical Results

In this section, we discuss the order of convergence in time of the proposed SBDF-ADI (8) and the standard SBDF (3) schemes. Then we discuss the performance of both methods in term of computational time and memory consumption. In all our numerical results, we will use the Mitchell–Schaeffer ionic model, given by:

$$I_{ion}(V_m, W) = \frac{1}{\tau_{in}}WV^2(1-V) - \frac{1}{\tau_{out}}V,$$

$$G(V_m, W) = \begin{cases} \dfrac{1-W}{\tau_{open}} & \text{for } V < v_{gate}, \\ -\dfrac{W}{\tau_{close}} & \text{for } V \geq v_{gate}. \end{cases}$$

The convergence in time is demonstrated using similar technique presented in [13] where a regular electrical cardiac wave is considered. The parameter values used provide a fast action potential upstroke and are given in Table 1.

Table 1: Parameters used in Mitchell–Schaeffer model

Constant	Value	Constant	Value
τ_{in}	0.05	τ_{out}	1
τ_{open}	95	τ_{close}	162
v_{gate}	0.13(mV)	$D_x = D_y$	0.001

We use the following discrete norms:

ICCS Camera Ready Version 2021
To cite this paper please use the final published version:
DOI: 10.1007/978-3-030-77977-1_43

$$e_{L^\infty} = \|V_h - V_r\|_{L^\infty} \text{ and } e_{L^2} = \|V_h - V_r\|_{L^2},$$

where V_r is a reference solution for the transmembrane potential obtained with a spatial discretization of 401 points ($M = 400$) in each direction and small time step ($N = 2 \times 10^6$). V_h is the numerical solution obtained with the same spatial mesh. In this example, the final time is $T = 330$. The result of this convergence test is presented in Figure 1, where it is clearly demonstrated the second order convergence for both methods. These numerical results can be supported by analytical work similar to the work presented in [13] to show that indeed both systems are of second order in time.

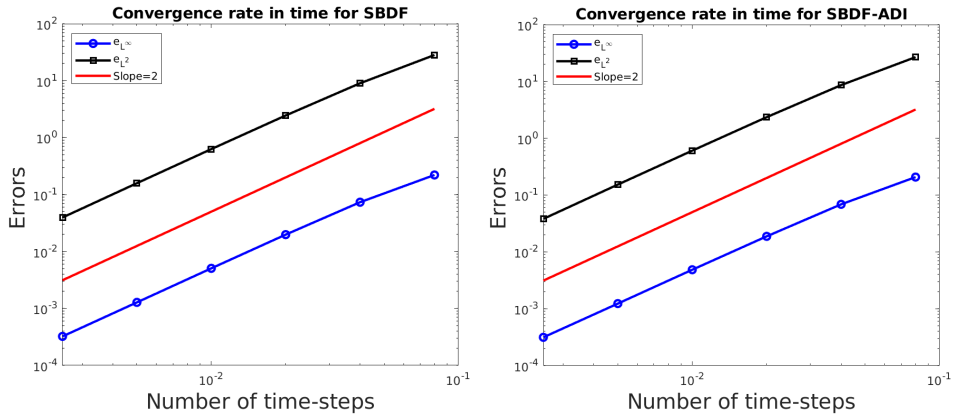

Fig. 1: Convergence order for SBDF and SBDF-ADI using Mitchell–Schaeffer model.

Now to demonstrate the performance of the proposed scheme SBDF-ADI (8), we investigate the computational time required for the simulations using both methods SBDF (3) and SBDF-ADI (8) for different values of space resolution (M) and for a fixed time step size ($N = 1.5 \times 10^4$). We consider a spiral wave dynamic in the Mitchell–Schaeffer model for the simulations. Different parameter values have been used in this case that are presented in Table 2.

Table 2: Parameters used in Mitchell–Schaeffer model

Constant	Value	Constant	Value
τ_{in}	0.3	τ_{out}	6
τ_{open}	120	τ_{close}	150
v_{gate}	0.13(mV)	$D_x = D_y$	0.001

ICCS Camera Ready Version 2021
To cite this paper please use the final published version:
DOI: 10.1007/978-3-030-77977-1_43

The spiral wave is obtained with a similar method presented in [15, 16], where the initial conditions are given as follows

$$V(x,y,0) = \begin{cases} 1 & \text{if } y \leq 4, \\ 0 & \text{otherwize,} \end{cases} \quad \text{and} \quad W(x,y,0) = \begin{cases} 0.75/2 & \text{if } x \leq 4.5, \\ 0.75/2 & \text{otherwize.} \end{cases}$$

The final time in this example is $T = 1500$. The time evolution of the transmembrane potential is presented in Figure 2.

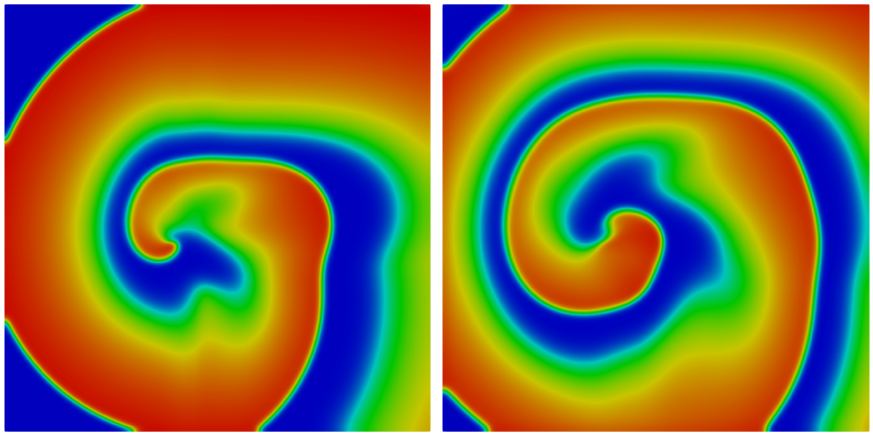

a) V at time $t = 600$ b) V at time $t = 900$

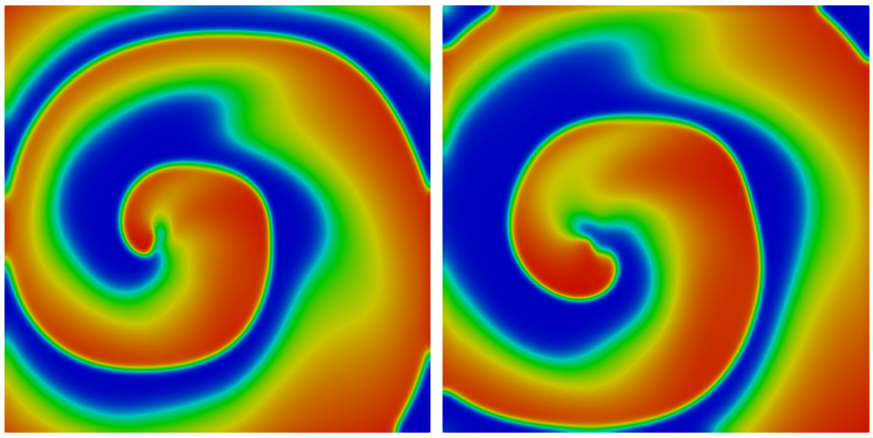

c) V at time $t = 1200$ d) V at time $t = 1500$

Fig. 2: Time evolution of spiral wave in Mitchell–Schaeffer model

ICCS Camera Ready Version 2021
To cite this paper please use the final published version:
DOI: 10.1007/978-3-030-77977-1_43

It is well known that this type of spiral wave requires extremely fine mesh resolution. Therefore, the computational time required for the simulation corresponding to various space resolutions, M, is presented in Figure 3. As can be seen, the computational time required by the proposed SBDF-ADI scheme is clearly lower than the required time for the standard SBDF method. This gain is mainly because of the size of the linear system involved in each method. In fact, the SBDF-ADI scheme involves matrices of size $(M+1, M+1)$, whereas the standard SBDF scheme requires a matrix of size $((M+1)^2, (M+1)^2)$. This also affects the memory requirement, where, for instance, in the case where $M = 600$ the memory required for the simulation using the SBDF-ADI is around 0.6 GB while the memory needed for SBDF is 1.6GB.

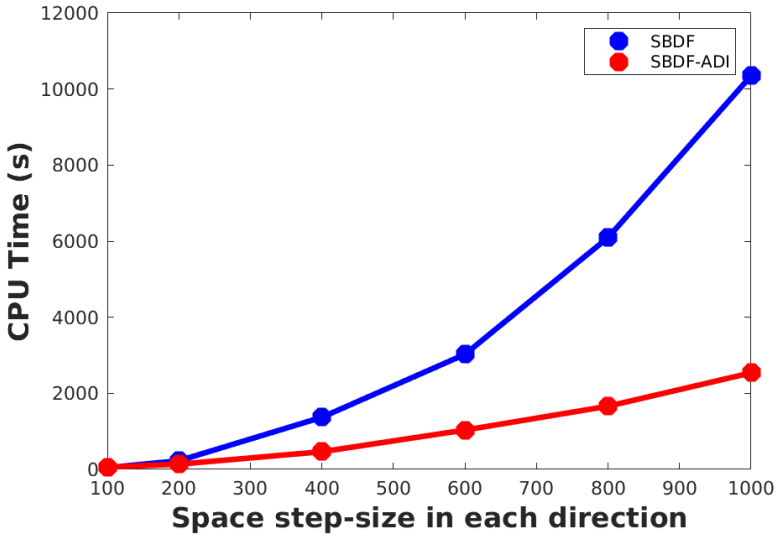

Fig. 3: Comparison of CPU time for SBDF and SBDF-ADI

4 Conclusion

In this paper, a second order alternating direction implicit finite difference method for both space and time was presented. The proposed ADI scheme was based on the semi-implicit backward differentiation formula. We showed that the proposed SBDF-ADI scheme provides the desired results while using less computational time. The advantage of the proposed SBDF-ADI scheme is that it can be extended to three-dimensional case, where the gain in computational resources will be clear as SBDF-ADI scheme involves matrices of size much smaller than

ICCS Camera Ready Version 2021
To cite this paper please use the final published version:
DOI: 10.1007/978-3-030-77977-1_43

the size of the matrix required for the standard SBDF scheme. The proposed SBDF-ADI scheme has also the advantage to be extended to include higher-order time and space difference schemes. This could provide accurate prediction of the cardiac electrical wave. Finite difference method has been previously used for solving the bidomain and monodomain models coupled with a realistic ionic model while using a computational geometry of a human heart. Therefore, the presented methodology can be extended to study realistic cardiac electrophysiology simulations which will be the subject of a future work.

References

1. Lucas A. Woodworth, Bariş Cansiz, and Michael Kaliske. A numerical study on the effects of spatial and temporal discretization in cardiac electrophysiology. *International Journal for Numerical Methods in Biomedical Engineering*, page e3443, 2021.
2. Thomas Roy, Yves Bourgault, and Charles Pierre. Analysis of time-stepping methods for the monodomain model. *Computational and Applied Mathematics*, 39:230:1–32, 2020.
3. Youssef Belhamadia. A time-dependent adaptive remeshing for electrical waves of the heart. *IEEE Transactions on Biomedical Engineering*, 55(2):443–452, 2008.
4. Youssef Belhamadia, André Fortin, and Yves Bourgault. Towards accurate numerical method for monodomain models using a realistic heart geometry. *Mathematical Biosciences*, 220(2):89–101, 2009.
5. J. Southern, G.J. Gorman, M.D. Piggott, P.E. Farrell, M.O. Bernabeu, and J. Pitt-Francis. Simulating cardiac electrophysiology using anisotropic mesh adaptivity. *Journal of Computational Science*, 1(2):82 – 88, 2010.
6. Christopher J. Arthurs, Martin J. Bishop, and David Kay. Efficient simulation of cardiac electrical propagation using high order finite elements. *Journal of Computational Physics*, 231(10):3946 – 3962, 2012.
7. Kevin Vincent, Matthew Gonzales, Andrew Gillette, Christopher Villongco, Simone Pezzuto, Jeffrey Omens, Michael Holst, and Andrew McCulloch. High-order finite element methods for cardiac monodomain simulations. *Frontiers in physiology*, 6:217:1–9, 2015.
8. Yves Coudière and Rodolphe Turpault. Very high order finite volume methods for cardiac electrophysiology. *Computers & Mathematics with Applications*, 74(4):684 – 700, 2017.
9. Jessica Cervi and Raymond J. Spiteri. A comparison of fourth-order operator splitting methods for cardiac simulations. *Applied Numerical Mathematics*, 145:227 – 235, 2019.
10. L. F. Pavarino and S. Scacchi. Parallel multilevel schwarz and block preconditioners for the bidomain parabolic-parabolic and parabolic-elliptic formulations. *SIAM Journal on Scientific Computing*, 33(4):1897–1919, 2011.
11. Yong Xia, Kuanquan Wang, and Henggui Zhang. Parallel optimization of 3d cardiac electrophysiological model using gpu. *Computational and Mathematical Methods in Medicine*, 2015:1–10, 2015.
12. Youssef Belhamadia, Thomas Briffard, and André Fortin. Application of parallel anisotropic mesh adaptation for solving monodomain cardiac model. *AIP Conference Proceedings*, 2343(1):130013, 2021.

ICCS Camera Ready Version 2021
To cite this paper please use the final published version:
DOI: 10.1007/978-3-030-77977-1_43

13. Youssef Belhamadia and Zeinab Rammal. Efficiency of semi-implicit alternating direction implicit methods for solving cardiac monodomain model. *Computers in Biology and Medicine*, 130:104187, 2021.
14. Marc Ethier and Yves Bourgault. Semi-implicit time-discretization schemes for the bidomain model. *SIAM J. Numerical Analysis*, 46:2443–2468, 2008.
15. Youssef Belhamadia, André Fortin, and Yves Bourgault. On the performance of anisotropic mesh adaptation for scroll wave turbulence dynamics in reaction–diffusion systems. *Journal of Computational and Applied Mathematics*, 271:233–246, 2014.
16. Youssef Belhamadia and Justin Grenier. Modeling and simulation of hypothermia effects on cardiac electrical dynamics. *PloS one*, 14(5):1–23, 2019.

ICCS Camera Ready Version 2021
To cite this paper please use the final published version:
DOI: 10.1007/978-3-030-77977-1_43